How to Cite: Turarbek, A.M., Abilkanova, F.Zh., & Uali, A.S. (2025). Development of Novel Wheat Waste-Derived Biochar and Its Potential in Pharmaceutical Wastewater Treatment. *Eurasian Journal of Chemistry, 30, 1(117), 76–88.* https://doi.org/10.31489/2959-0663/1-25-2

CHEMICAL TECHNOLOGY

Article

Received: 27 November 2024 | Revised: 15 January 2025 |
Accepted: 19 February 2025 | Published online: 13 March 2025

UDC 661.183.2, 620.181.4 https://doi.org/10.31489/2959-0663/1-25-2

Ayazhan M. Turarbek[1], Farida Zh. Abilkanova[2], Aitolkyn S. Uali[1*]

[1]L.N. Gumilyov Eurasian National University, Astana, Kazakhstan;
[2]Karaganda Industrial University, Temirtau, Kazakhstan
*(*Corresponding author's e-mail: uali_as@enu.kz)*

Development of Novel Wheat Waste-Derived Biochar and Its Potential in Pharmaceutical Wastewater Treatment

The rising concentration of pharmaceuticals in wastewater presents significant environmental and health challenges. This study aims to develop an iron (III)-activated carbon-enriched material derived from local agricultural plant waste to effectively remove pharmaceutical contaminants. The research investigates the material's composition, structure, morphology, and adsorption capacity of the material, focusing on wheat waste-derived biochar. The synthesis process includes an initial carbonization, chemical modification with FeCl3 using the wet impregnation method, and a second carbonization and washing step. The resulting carbonaceous material was characterized using the CHNS elemental analyzer, FTIR, XRD and SEM-EDX spectroscopic techniques. The results indicate the formation of a carbonaceous material with a carbon content of 77.09 %, enriched with a highly crystalline graphite phase and a porous structure containing iron (II, III) oxides. Notably, this sorbent efficiently reduced the ibuprofen concentration, with a sorption capacity of 433 mg•g^{-1}. Among the pseudo-first-order (PFO), pseudo-second-order (PSO), intraparticle diffusion and Elovich models used to describe the adsorption kinetics, the PSO model (types 1-2) fits successfully, indicating chemisorption-controlled kinetics. This study highlights the potential for converting agricultural waste into a carbonaceous material with improved structure and morphology, and demonstrates its high efficacy in purifying water from pharmaceutical contaminants.

Keywords: waste wheat, carbonization, biochar, activated carbons, iron oxides, adsorption, ibuprofen, kinetic models, pseudo-second-order kinetic model.

Buketov University

Introduction

Carbonaceous materials obtained from agricultural residues have great potential for development of sustainable technologies. Recent studies have demonstrated that biochar is not only applicable but also under development as an effective sorbent [1–4], electrode-active material [5–8], and catalyst [9–11]. These studies reveal the potential of waste streams to contribute to circular bioeconomy strategies that transform resource use, an issue that will highlight the evolving environment of sustainable practices [12].

Currently, there is an increasing in demand for active pharmaceutical compounds, and therefore, the pharmaceutical industry continues to increase the production of drugs. As a result, discharges of industrial effluents are regularly increasing, raising serious concerns about their harmful effects on human health and the aquatic environment. Ibuprofen (IBU), 2[4-(2-methylpropyl)phenyl]propanoic acid, is a globally recognised anti-inflammatory drug, widely used in medical practice as an antipyretic, analgesic and anti-inflammatory agent [13–15]. In the US, UK, and Poland, ibuprofen consumption is approximately 300, 162 and 58 tons per year [16]. It is metabolised in the body and the environment to form ibuprofen derivatives. It has been found that when ibuprofen is released into the environment it is initially degraded to form hydrox-

 © 2025 The Authors. This is an open access article under the CC BY-NC-ND license (http://creativecommons.org/licenses/by-nc-nd/4.0/)

ylated ibuprofen and ibuprofen carboxylic acid; benzoquinone, quinone and catechol-like compounds are also formed during the degradation of ibuprofen [17]. Chorpa and Kumar have proposed a way for the degradation of ibuprofen, indicating various intermediate products formed during degradation (Fig. 1) [18].

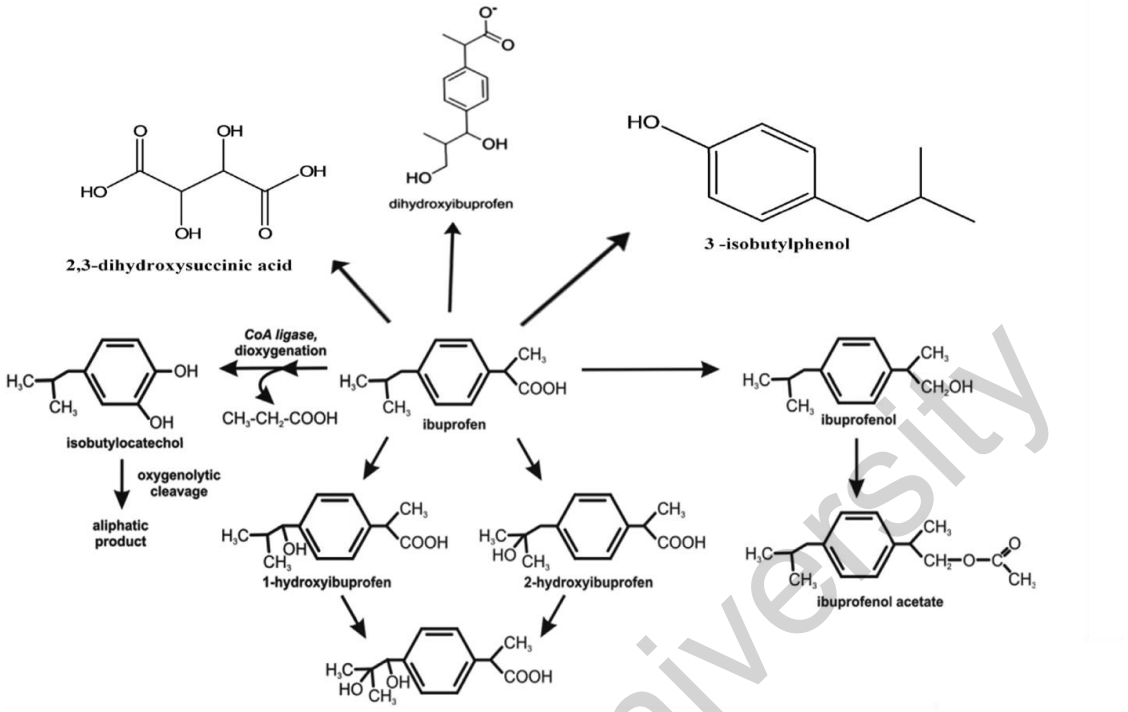

Figure 1. A way of ibuprofen degradation with various intermediate products.
Reprinted from Ref. [18] with permission under the license CC BY-NC-ND 4.0 International

Therefore, pharmaceutical contaminants need to be removed from the aquatic environment. As reported, electrocoagulation [19], oxidation [20, 21], membrane filtration [22], and adsorption [21] are recommended. Although these methods are effective in achieving high percentages of IBU removal, they also have drawbacks, including energy consumption and cost. Herein, adsorption is the most promising water treatment method in terms of effectiveness and environmental sustainability. Moreover, utilising waste biomass further reduces the price of this purification process.

According to the Food and Agriculture Organization of the United Nations [23], Kazakhstan is a leading wheat exporter, producing 16.4 million tonnes of wheat in 2022. This extensive production generates substantial biowaste (straw, husk, *etc.*). However, the literature review revealed limited studies utilising waste wheat in polluted water treatment; no data describing local biochar produced from wheat waste biomass. A critical aspect of the relevance and practical significance of this study is the proposal of a carbon sorbent from domestic agricultural waste to purify water bodies from ibuprofen. This study aims to produce biochar derived from local biowaste and test its adsorption capacity towards ibuprofen in an aqueous solution. It is expected that biochar derived from wheat waste will have an enhanced adsorption capacity for ibuprofen compared to other materials.

Experimental

2.1 Chemicals and Materials. All chemicals (1 % $FeCl_3$, 0.1 M NaOH solution) were analytical grade. DI water was used as the solvent. Ibuprofen sodium salt (Sigma Aldrich) was used to prepare its working solution.

2.2 Preparation of Biochar. Wheat wastes were used as an initial substance to prepare biochar using a three-stage treatment consisting of the first carbonisation (temperature of 600 °C, heating rate of 20 °C/min, 1 h under the Ar atmosphere), chemical modification (agent of 1 % $FeCl_3$ solution, solid-to-liquid ratio of 1/10 in wt.%) and the second carbonisation (under the same conditions as in the first stage). The chemical modification stage was conducted by immersing the intermediate into the agent's solution for 24 h at room temperature (21 °C±0.5 °C). After the second carbonization, the product was washed with hot water

Buketov University

(90 °C±3 °C) several times until a neutral pH value and dried at a temperature of 115 °C till its weight was constant. The final product — biochar — was then used in materials characterization and sorption tests as a sorbent.

2.3 Determination of the Ash Content. The biochar samples were oven-dried at 105 °C and then heated in a covered crucible in a muffle furnace at 750 °C for 6 h. The mass of material remaining after incineration refers to ash [24]. The ash test was conducted in three parallels to evaluate the standard deviation (SD).

2.4 Materials Characterization. The CHNS test (carbon (C), hydrogen (H), nitrogen (N) and S (sulfur)) was conducted using the Unicube organic elemental analyser. The % oxygen is obtained by recording the difference between 100 and the CHNS+ash content (in %) [24]:

$$O_{subs} = 100 - (C + H + N + S + A),$$

where C, H, N, S and A are the contents (in %) of carbon, hydrogen, nitrogen, sulfur and ash, respectively.

The BET analysis (low-temperature nitrogen adsorption) on the BSD-66OS A3 apparatus evaluated the biochar's porous structure and specific surface area. The samples were prepared at 200 °C and maintained at a residual pressure of at least 0.001 bar. Nitrogen adsorption and desorption isotherms were recorded at 77 K, utilising liquid nitrogen in the relative pressure range from 0.005 to 0.991 bar. Standard analysis of the results was performed using the Barrett-Joyner-Halenda (BJH) method, which employs a conventional cylindrical pore model. This analysis included the calculation of several parameters: the total surface area (ΣS), the micropore surface area (μS) using the Brunauer-Emmett-Teller (BET) method, the total pore volume (ΣV), the micropore volume (μV), and the average pore diameter (D_{av}). These calculations considered both micro- and mesopores and utilised the DFT approach.

The FTIR spectroscopic measurements were carried out using an Alpha II FTIR spectrometer (Bruker) operating at a frequency range between 4000 and 400 cm^{-1} at room temperature. The samples were prepared by mixing KBr and the BC sample (ratio 99.5 %:0.5 %) by weight and pressed into a disc before analysis, which consisted of 32 scans with a resolution of 1 cm^{-1}.

The SEM-EDX analysis (n=3) used the Phenom ProX Scanning Electron Microscope (Thermo Scientific) (high voltage of 15kV) with the BSD detector.

X-ray diffraction patterns were recorded using a D8 Advance Eco diffractometer (Bruker) in Bragg-Brentano geometry in the angular range of 14...100° (2θ) (step 0.05) at room temperature. An X-ray source was a copper tube with radiation (λ = 1.54060 Å).

2.5 Spectrophotometric Analysis of Ibuprofen. For the spectrophotometric determination of an aqueous solution of IBU, its powder was dissolved in a previously prepared 0.1 M NaOH solution and shaken for about 10 min. After filtration, the aqueous solution of ibuprofen was subjected to spectrophotometric analysis. Spectrophotometric measurements were done according to [25] at a wavelength of 273 nm on a spectrophotometer Specord 250. A calibration curve is given in Figure 2.

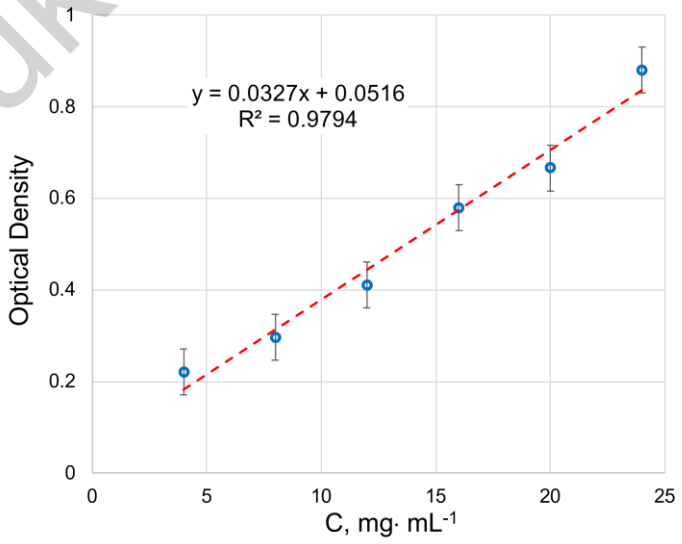

Figure 2. Optical density – concentration dependence for spectrophotometric analysis of IBU

Buketov University

2.6 Ibuprofen Adsorption Tests. Adsorption tests were carried out at static conditions according to [26]. In adsorption tests, a biochar sample (10 mg) was immersed in an IBU solution (20 ml). All adsorption tests (n = 3) were conducted at a controlled temperature **(**21 °C±0.5 °C). The total adsorption time was up to 60 min. The liquid phase was then separated by filtration. To determine the residual concentration of IBU in the liquid phase, the optical density was measured at 340 nm wavelength. The adsorption value (a) was calculated as follows:

$$\alpha = \frac{\nu}{m} = \frac{\nu(C_0 - C)}{m},$$

where ν is a solution volume on which adsorption is carried out, L; C_0 is the initial concentration of I (mol·L^{-1}); C is the residual concentration of IB (mol·L^{-1}), and m is the weight of sorbent (g).

Results and Discussion

3.1 Material Characterisation of Biochar. Table 1 demonstrates the CHNS results and waste wheat-derived biochar's ash and oxygen content.

Table 1

Elemental composition of biochar, ashness and the H/C, O/C ratios

Initial material	C, %	H, %	N, %	S, %	A, %	O_{subs}, %	H/C	O/C	Ref.
Rapeseed wastes	72.60	4.90	6.70	0.50	–	15.30	0.07	0.21	[27]
Palm kernel shell	47.28	5.32	0	0	–	47.40	0.11	1	[28]
Rice husk	41.11	4.87	0.80	0.04	–	53.17	0.12	1.29	[29]
Coconut fibers	44.89	5.19	0.86	0.03	–	48.64	0.12	1.08	[29]
Durian peel	39.30	5.90	1.00	0.06	4.84	53.74	0.15	1.37	[30]
Waste wheat	77.09±0.22	1.91±0.02	4.15±0.04	0	12.12±0.20	4.71±0.38	0.02	0.06	Present study

As shown in Table 1, wheat-derived biochar has the highest carbon content of 77.09 % compared to rice husks, with a carbon content of 41.11 % [29]. Another noticeable difference is the O content, which is 53.74 % for durian-derived biochar, which is ≈13 times higher than wheat-derived biochar and 3-4 times higher for rapeseed residue. The lower the O/C and H/C atomic ratios, the higher the degree of aromaticity and stability of the carbonised material [31]. The relatively low value of the H/C ratio, 0.02, might be attributed to the elimination of dehydration and dehydrogenation reactions and the cleavage and cracking of weak hydrogen bonds during conversion within the biochar [32]. The O/C ratio lowers if a high degree of carbonisation occurs by removing oxygen through dehydration and decarboxylation reactions [33]. These data have revealed that biochar might demonstrate long-term chemical stability.

Regarding the porosity of biochar, the porous structure could be derived from the structure present in the raw biomass or was formed during the devolatilization process of gasification. In [34], wheat bran biochar has a lower specific surface area (SSA) of 25 m^2·g^{-1}. In comparison, Vaghela *et al.* [35] reported that wheat straw biochar produced at 600 °C has a SSA of approximately 70.12 m^2·g^{-1}. Zhu *et al.* [36] highlighted the contribution of iron oxide particles to the biochar pores. According to the BET analysis, the SSA of biochar was 227.84 m^2·g^{-1} with the pore volume distribution as follows: micropores (0.35–2 nm), mesopores (2–10 nm and 10–50 nm) and macropores (50–200 nm) are 70.48 %, 22.45 %, 3.42 % and 0.65 %, respectively. The increased SSA is most likely due to the contribution of iron oxides.

The presence of iron-containing compounds in the production of activated carbon reduces the temperature required for cellulose hydrolysis, resulting in a notable depolymerisation reaction that produces a significant amount of low-molecular-weight hydrocarbons. Iron chlorides disrupt the glycosidic bonds in cellulose at pyrolysis temperatures between 200 °C and 300 °C, simultaneously releasing water molecules from the hydrated salt and generating glucose monosaccharides. Within this temperature range, the hydrated iron chloride decomposes into amorphous FeOOH through specific chemical reactions [36]:

$$FeCl_3 + 2H_2O \leftrightarrow FeOCl \cdot H_2O + 2HCl \quad (1)$$

$$FeOCl \cdot H_2O \leftrightarrow FeOOH + HCl \quad (2)$$

Buketov University

The second stage, occurs at pyrolysis temperatures above 330 °C. As the activation temperature increases, glucose molecules successively undergo ring opening, dehydration, and cyclisation into 5-hydroxymethylfurfural, which, after decarbonylation, is converted to furfural [37]. With increasing temperature, FeOOH first decomposes into Fe_2O_3, then the carbon surface is reduced, and Fe_3O_4 is formed via the following chemical reactions [37]:

$$2FeOOH \leftrightarrow Fe_2O_3 + H_2O \quad (3)$$

$$3Fe_2O_3 + C \leftrightarrow 2Fe_3O_4 + CO \quad (4)$$

Iron oxides are crucial in catalysing microporosity formation within the carbon matrix. Overall, porous activated carbons are formed in the presence of iron species with highly stable Fe bound to their surface [38].

The EDS mapping of biochar's surface demonstrated its elemental composition and distribution (Fig. 3).

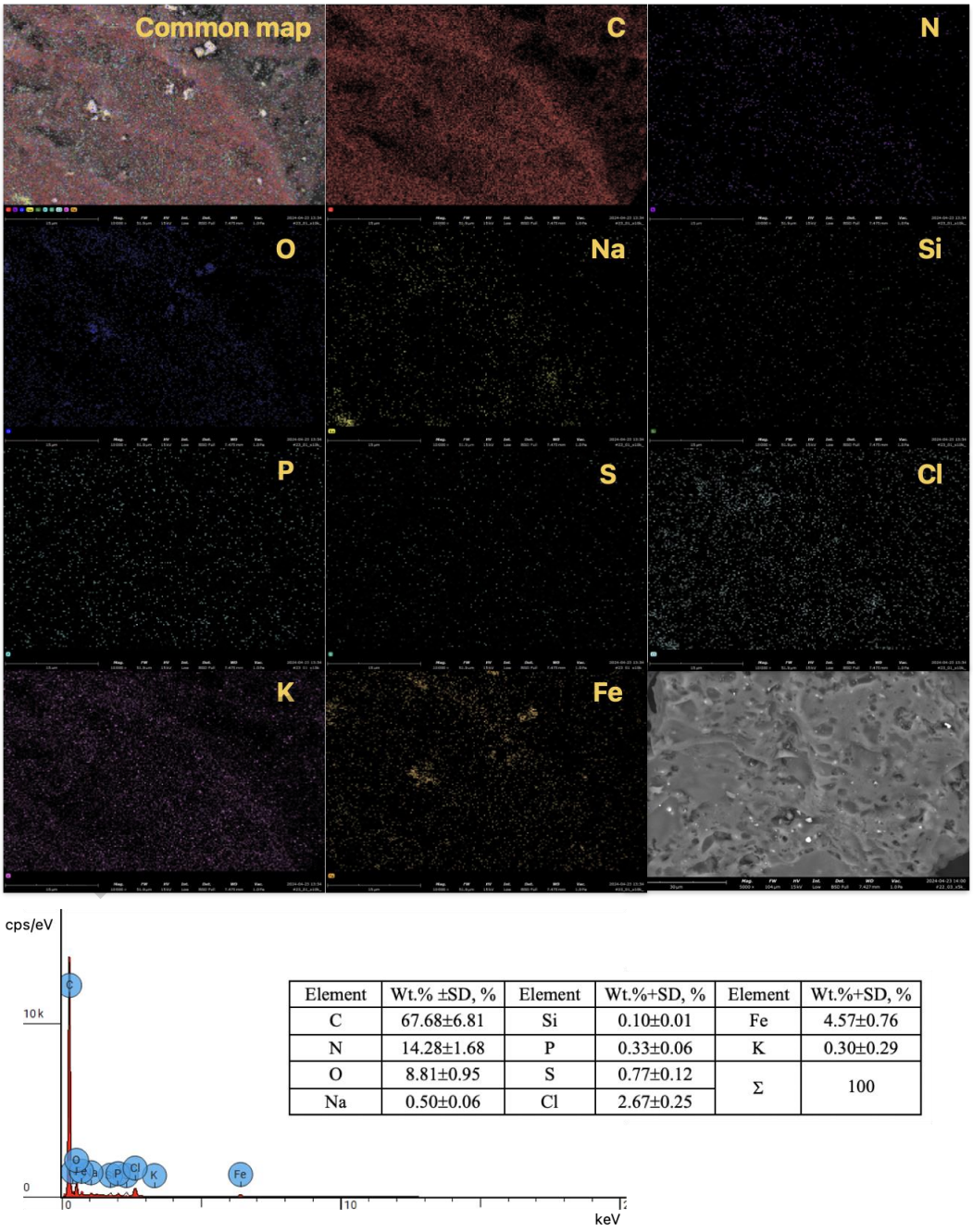

Element	Wt.% ±SD, %	Element	Wt.%+SD, %	Element	Wt.%+SD, %
C	67.68±6.81	Si	0.10±0.01	Fe	4.57±0.76
N	14.28±1.68	P	0.33±0.06	K	0.30±0.29
O	8.81±0.95	S	0.77±0.12	Σ	100
Na	0.50±0.06	Cl	2.67±0.25		

Figure 3. EDS mapping pictures and elemental content of biochar's surface

The EDS maps indicated that biochar produced from waste wheat is rich in elements such as carbon, nitrogen, and oxygen, which are relatively evenly distributed; however, some areas show higher or lower concentrations of these elements. In contrast, iron is concentrated in specific areas, particularly within pores, as suggested.

The XRD study demonstrates that biochar has a semicrystalline structure (Fig. 4). This is indicated by a broad signal between 20° and 30°, typically characteristic of the stacking structure of aromatic layers associated with highly crystalline graphite (graphite 002) [39, 40].

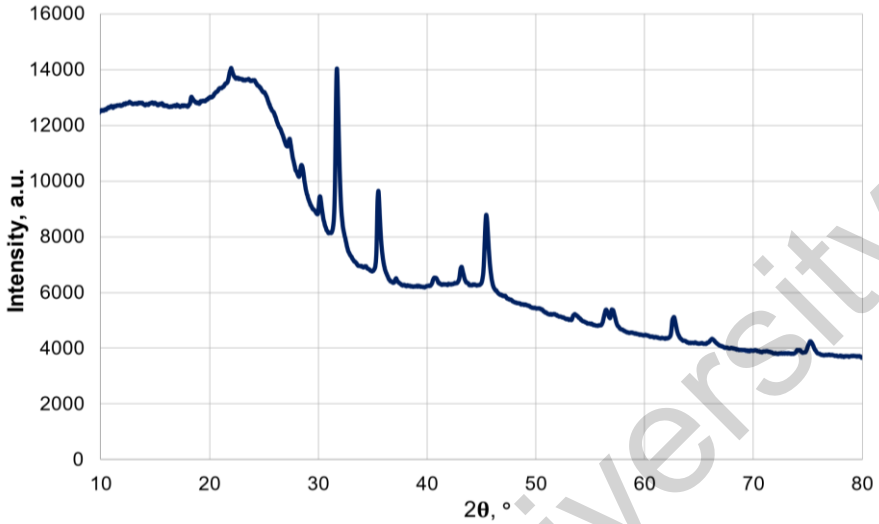

Figure 4. XRD spectrum of biochar (final product)

The sharp diffraction peaks at 32°, 35°, and 45° could be attributed to the plane interlayer reflections $Fe_2O_3 \cdot FeO$ [41]. According to the database of the Joint Committee on Powder Diffraction Standards database (JCPDS #75-0449), Fe_3O_4 appeared at 30.5°, 35.7° and 43°, which are identical to crystal plane index (220), (331) and (400) [42]. In [43], characteristic bands of hematite crystals are located at 2θ of 32.0°. Based on this, it could be suggested that iron (II, III) oxide particles were successfully injected into the carbon matrix during the modification-carbonization process.

The FTIR spectroscopy experiment was performed to identify the functional groups of waste wheat-derived biochar (Fig. 5).

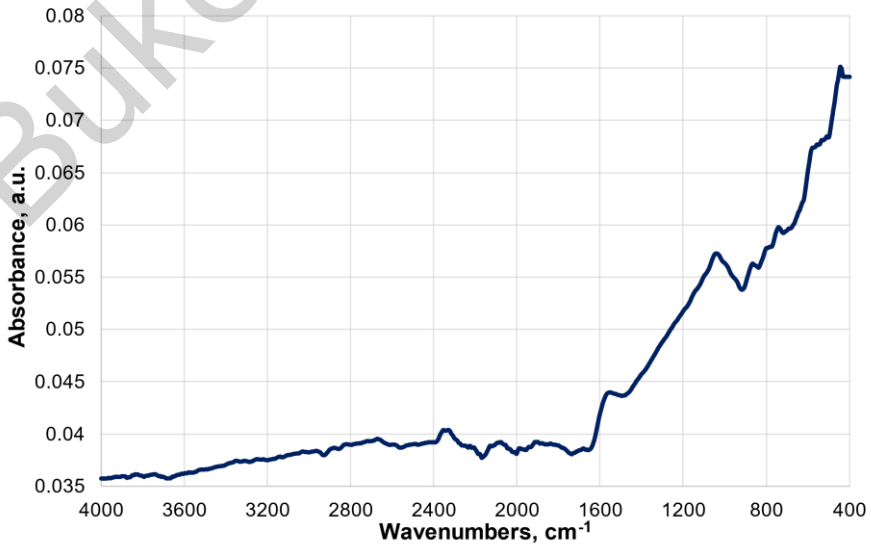

Figure 5. FTIR spectrum of biochar (final product)

Buketov University

Biochar's functional groups matched those of the references [44–46]. The spectral analysis shows that the three-stage treatment effectively removes or alters the functional groups present in the carbon material, resulting in a more graphitic carbon structure with fewer detectable functional groups than the FTIR spectrum of the intermediate biochar product after the first carbonisation stage, as illustrated in Figure S1 and Table S1 (see the supplemental file). For example, a peak at 1536 cm^{-1} may be attributed to the C=C stretching in the aryl double bond [47]; another peak at 1015 cm^{-1} likely corresponds to the C–OC or C–OH bonds [48]. Additionally, a peak at 580 cm^{-1} might be assigned to Fe–O vibrations [49, 50].

3.2 Ibuprofen Adsorption on Waste Wheat-Derived Biochar. The experimental data (Fig. 6) show that the adsorption process reached equilibrium after 10 min, and then the adsorption value remained stable over time. The readily accessible active sites cause the initial rapid adsorption, while the plateau indicates equilibrium with IBU molecules entering and exiting the active sites at the same rate. The same behaviour has previously been detected for ibuprofen adsorption using commercial activated carbons and polymeric resin [51], cellulosic biomass [52], and sonicated activated carbons [53].

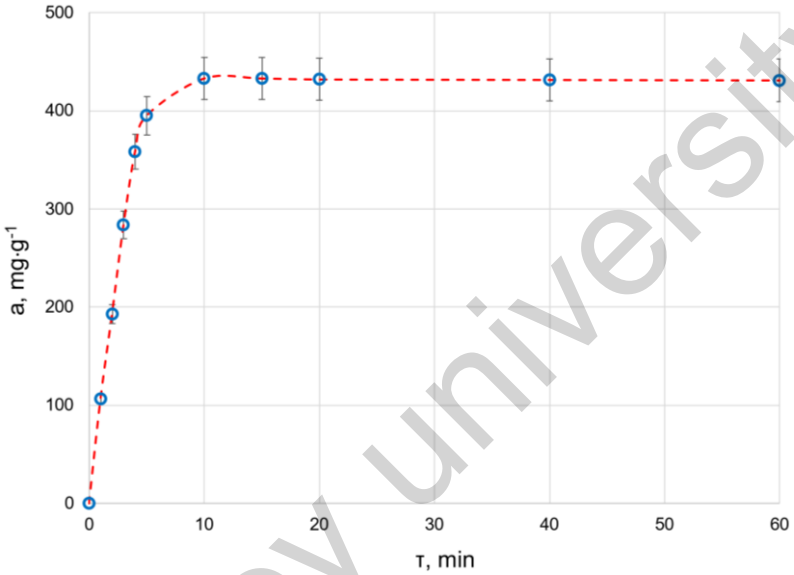

Figure 6. Adsorption kinetic curve of ibuprofen onto biochar

Buketov university

Comparing the adsorption capacity of the current sorbent with the references shows that, in some cases, the ibuprofen adsorption capacity is higher for the biochar of interest (Table 2).

Table 2

Comparison of waste wheat-derived biochar with others

Initial biomass	Type of activation/modification	SSA, $m^2 \cdot g^{-1}$	Ibuprofen uptake capacity, $mg \cdot g^{-1}$	Kinetic model	Ref.
Sugarcane bagasse	Chemical	557.00 (for raw biochar)	13.51	PSO	[54]
	Steam		11.90	PSO	
Bovine bones	Chemical (ZnAl)	170.00 $cm^2 \cdot g^{-1}$ (external)	1032.81	n.r.*	[55]
Chrysanthemum wastes	Magnetic	194.00	167.00	PSO	[56]
	Non-magnetic	220.00	140.00	PSO	
Rice husk	Chemical (H_3PO_4)	n.r.*	239.80	PSO	[57]
Babassu coconut shell	Ultrasound	732.00	134.00	PSO	[58]
Recycled textile materials	Steam	710.00	53.90	Elovich	[59]
Sunflower seed husk	Chemical (H_3PO_4)	378.80	251.10	Elovich	[60]
Cork powder	Both chemical/physical	1060.00	393.40	PSO	[61]
Wheat husk	Chemical ($FeCl_3$)	227.84	433.00	PSO	Present study

Note: * — not reported.

It is known that higher SSA generally correlates with better adsorption capacity, but other factors such as pore size distribution and surface functional groups also play a crucial role [62]. These differences in the surface and porosity of resulting biochars may also be due to the experimental preparation conditions, including pyrolysis temperature and time, or the additional activation steps, such as using gas or steam. It is worth noting that, according to the European Biochar Certificate Standard (EBC), biochars should have an SSA larger than 150 $m^2 \cdot g^{-1}$ [56, 63].

The adsorption kinetics describes the solute uptake rate, and its knowledge is essential for a better understanding of the reaction mechanism and designing appropriate adsorption technologies. It is known that the kinetic model is fitted best if there are three conditions to be satisfied: 1) a reasonable match of experimental and calculated values of adsorption uptake, 2) the regression value (R^2) should be close to 1, 3) the values of chi-square test (χ^2) and the sum of the square of the error (SSE) should be minimum. Pseudo-first order (PFO) and pseudo-second-order (PSO) kinetic equations [64], as well as the intraparticle diffusion model and Elovich model, were tested to fit the experimental data obtained from the batch experiments (Table 3), where $k_1\left[\min^{-1}\right]$, $k_2\left[\mathrm{g}\cdot\mathrm{mg}^{-1}\cdot\min^{-1}\right]$ are the PFO and PSO rate constants, q_e $[\mathrm{mg}\cdot\mathrm{g}^{-1}]$ and q_t $[\mathrm{mg}\cdot\mathrm{g}^{-1}]$ are the adsorbate uptake at equilibrium and at time *t*, respectively, K_{Diff} $[\mathrm{mg}\cdot\mathrm{g}^{-1}\cdot\min^{-1/2}]$ is a measure of diffusion coefficient, C $[\mathrm{mg}\cdot\mathrm{g}^{-1}]$ is intraparticle diffusion constant, α $[\mathrm{mg}\cdot\mathrm{g}^{-1}\cdot\min^{-1}]$ is the Elovich initial adsorption velocity, β $[\mathrm{g}\cdot\mathrm{mg}^{-1}]$ is the Elovich constant, R^2 is the regression coefficient.

Table 3

Kinetic models for the ibuprofen adsorption parameters onto biochar

PFO	k_1	q_e	R^2
$\ln(q_e - q_t) = \ln(q_e) - k_1\tau$	0.0711	67.26	0.4203
PSO, type 1	k_2	q_e	R^2
$\frac{\tau}{q_\tau} = \frac{1}{k_2 q_e^2} + \left(\frac{1}{q_e}\right)\tau$	0.0015	454.54	0.9975
PSO, type 2	k_2	q_e	R^2
$\frac{1}{q_\tau} = \left(\frac{1}{k_2 q_e^2}\right)\left(\frac{1}{\tau}\right) + \left(\frac{1}{q_e}\right)$	0.0073	588.23	0.9967
PSO, type 3	k_2	q_e	R^2
$\frac{\tau}{q_\tau} = k_2 q_e^2 - k_2 q_e q_t$	0.0005	564.06	0.6574
PSO, type 4	k_2	q_e	R^2
$q_\tau = q_e - \left(\frac{1}{k_2 q_e}\right)\frac{q_\tau}{\tau}$	0.0004	962.68	0.6574
Intraparticle diffusion	C	K_{Diff}	R^2
$q_\tau = K_{Diff}\tau^{1/2} + C$	225.38	36.76	0.4836
Elovich	α	β	R^2
$q_\tau = \frac{1}{\beta}\ln(\alpha\beta\tau + 1)$	286.71	0.0052	0.7344

Firstly, the PFO model calculates the kinetic parameters k_1 and q_e [65]. The k_1 value describes how quickly the adsorption equilibrium is reached in the studied system. However, since the adsorption rate is related to k_1 and α values; they must be considered together. For example, if the value of k_1 is low and the $q_e - q_t$ value is high, it indicates slow adsorption. Generally, the PFO model corresponds to a high initial adsorbate concentration, and adsorption is not controlled by adsorption at the active sites. Sometimes, the PFO model may reflect external/internal diffusion. Similar to the PFO-k_1 rate constant, the PSO-k_2 rate constant is also used to describe the rate of adsorption equilibrium [66]. This model accounts for some adsorp-

Buketov University

tion processes requiring more prolonged time to fill the adsorption sites [67]. The adsorption rate is assumed to be affected by the interaction of adsorption sites on the adsorbent surface with the adsorbent throughout the adsorption process. The intraparticle diffusion model describes a transport process where species move from the bulk solution to the solid phase (sorbent) [68]. It is more applicable for porous adsorbents. Although the Elovich model has been developed to describe interactions between a solid/gas interface, it has effectively defined processes that occur on a solid/liquid interface [69]. It is reported that the model considers that the actual solid surface is energetically heterogeneous and that the desorption process and interactions between adsorbed species do not significantly affect the adsorption kinetics.

In this study, the sorption kinetics may be described by a PSO model due to the values of regression coefficient (R^2) and closeness of experimental and theoretical adsorption capacity (q_e) (Table 3). According to Ghaedi *et al.* [70], the fit of the PSO model indicates that the process is controlled by chemisorption or ion exchange due to the porous surface of the carbonaceous materials. Also, the fitting of this model might be explained by the occurrence of multilayer adsorption and vertical packing of adsorbate in active sites. Another study [71] revealed that the fit of the experimental data to the PSO model indicates the adsorption of the pollutant by two active sites simultaneously. Also, the chemisorption might be the limiting stage of the kinetic processes when valence bonds between the sorbate and the adsorbent are shared or exchanged.

Various key processes are involved in the adsorption of ibuprofen onto biochar, including hydrogen bonding, chemical adsorption, pore filling, electrostatic interactions, and π-π stacking. Primarily, it's essential to consider the surface functional groups, such as carboxylic and hydroxylic, that facilitate hydrogen bonding and enhance adsorption. Additionally, the PSO kinetic model is likely indicative of chemisorption. Lastly, the pores present are adequately sized to accommodate ibuprofen. According to [64], the predicted size of the molecular structure of ibuprofen is 1.03 nm×0.52 nm×0.43 nm. Considering the pore volumes and sizes, alternative pore filling is also possible for ibuprofen held by biochar. Altogether, these interactions facilitate the effective capture of ibuprofen within the porous structure of biochar.

3.3 Spent Adsorbent Disposal. Proper disposal of used adsorbents is essential due to significant environmental concerns. The World Health Organization (WHO) has issued important guidelines titled "Guidelines for Safe Disposal of Unwanted Pharmaceuticals in and after Emergencies" [72], which emphasise that adsorbents infused with ibuprofen can be disposed of safely and responsibly by following established pharmaceutical disposal methods. This approach protects public health and helps safeguard the environment from potential contaminants. The adsorption of ibuprofen onto biochar is predominantly irreversible, emphasising its effectiveness as a long-term solution for treating water contaminants. Once ibuprofen is adsorbed, it remains securely bound to the sorbent surface, making it an ideal candidate for reliable pollution management. Incineration is a preferred disposal technique for spent adsorbents, ensuring the destruction of any residual pharmaceuticals. Since ibuprofen-loaded biochar boasts a high calorific value, it provides an eco-friendly alternative to coal and allows energy recovery through incineration or gasification for syngas production. Moreover, various other disposal methods, such as regeneration, have also been explored, further enhancing the viability of biochar in sustainable waste management.

Conclusions

The findings of this study indicate that local agricultural waste, such as wheat residue, can be effectively converted into biochar infused with a mixture of iron (II, III) oxides. This biochar has a unique composition, rich in carbon (77.09 %), with a specific surface area of 227.84 $m^2\ g^{-1}$, predominantly characterised by micropores (70.48 %). Notably, the material has a high adsorption capacity for ibuprofen, reaching a sorption capacity of 433 $mg{\cdot}g^{-1}$. Kinetic studies have shown that a pseudo-second-order model describes the adsorption process. Waste wheat presents a promising alternative for the development adsorbents to remove ibuprofen from aqueous solutions. This innovative approach tackles the challenge of agricultural waste disposal and provides a cost-effective and sustainable solution to improve water quality. The use of this method makes a significant contribution to environmental protection and effective water treatment strategies.

Supporting Information

The Supporting Information is available free at https://ejc.buketov.edu.kz/index.php/ejc/article/view/212/180

Buketov University

*Author Information**

**The authors' names are presented in the following order: First Name, Middle Name and Last Name*

Ayazhan Meirbekkyzy Turarbek — Student, L.N. Gumilyov Eurasian National University, K. Munaitpassov st., 13, 010000, Astana, Kazakhstan; e-mail: turarbekayazhan@gmail.com, https://orcid.org/0009-0009-6174-2837

Farida Zhumageldyevna Abilkanova — Master of Science, Karaganda Industrial University, Republic Avenue, 30, 101400, Temirtau, Kazakhstan; e-mail: f.abilkanova@tttu.edu.kz, https://orcid.org/0000-0002-6894-5276

Aitolkyn Sailaubekkyzy Uali (*corresponding author*) — Candidate of Chemical Sciences, Assoc. Professor, L.N. Gumilyov Eurasian National University, K. Munaitpassov st., 13, 010000, Astana, Kazakhstan; e-mail: uali_as@enu.kz, https://orcid.org/0000-0002-5851-6566

Author Contributions

The manuscript was written through contributions of all authors. All authors have given approval to the final version of the manuscript. CRediT: **Ayazhan Meirbekkyzy Turarbek** — investigation, formal analysis, writing-original draft, **Farida Zhumageldyevna Abilkanova** — formal analysis, visualisation, **Aitolkyn Sailaubekkyzy Uali** — supervision, data curation, methodology, review & editing.

Conflicts of Interest

The authors declare no conflict of interest.

Notes

A graphical abstract was created in BioRender. Uali, A. (2025) https://BioRender.com/k69i500

References

1 Amerkhanova, Sh.K., Shlyapov, R.M., Uali, A.S., & Tatibayeva, M.S. (2016). The concentration of cadmium (II), lead (II) and mercury (I, II) ions by adsorption on the wood-modified sorbent. *Bulletin of the Karaganda University. Chemistry series*, 4(84), 38–43. https://doi.org/10.31489/2016ch4/38-43

2 Amerkhanova, Sh.K., Uali, A.S., & Abilkanova, F.Zh. (2017). Evaluation of the thermal stability of sorbents based on modified active carbons. *Bulletin of the Karaganda University. Chemistry Series*, 2(86), 42–46. https://doi.org/10.31489/2017ch2/42-46

3 Amerkhanova, Sh., Uali, A., Shlyapov, R., & Yerkin, K. (2022). Evaluation of adsorption properties of carbon material obtained from a pinecone in relation to nitrogen. *Bulletin of the L.N. Gumilyov Eurasian National University. Chemistry. Geography. Ecology Series, 139*(2), 7–17. https://doi.org/10.32523/2616-6771-2022-139-2-7-17

4 Vinayagam, V., Murugan, S., Kumaresan, R., Narayanan, M., Sillanpää, M., Viet N Vo, D., Kushwaha, O. S., Jenis, P., Potdar, P., & Gadiya, S. (2022). Sustainable adsorbents for the removal of pharmaceuticals from wastewater: A review. *Chemosphere, 300*, 134597. https://doi.org/10.1016/j.chemosphere.2022.134597

5 Amerkhanova, Sh., Shlyapov, R., Uali, A., & Belgibaeva, D. (2022). Prospects of application of iron-containing carbon-paste electrode in electrochemical analysis. *Materials Today Proceedings, 49*, 2532–2536. https://doi.org/10.1016/j.matpr.2021.05.437

6 Kumar, Y.A., Rai, R.K., Akbar, M.A., Verma, V., Singh, S.K., & Srivastava, S.K. (2024). The landscape of energy storage: Insights into carbon electrode materials and future directions. *Journal of Energy Storage, 86*, 111119. https://doi.org/10.1016/j.est.2024.111119

7 Rahman, M.Z., Edvinsson, T., & Kwong, P. (2020). Biochar for electrochemical applications. *Current Opinion in Green and Sustainable Chemistry, 23*, 25–30. https://doi.org/10.1016/j.cogsc.2020.04.007

8 Rawat, S., Wang, C.-T., Lay, C.-H., Hotha, S., & Bhaskar, T. (2023). Sustainable biochar for advanced electrochemical/energy storage applications. *Journal of Energy Storage, 63*, 107115. https://doi.org/10.1016/j.est.2023.107115

9 Lei, X., Zhang, X., Zheng, Y., Xiang, Y., Tan, P., Luo, Z., Huang, H., Pan, B., Zhu, Y., Hu, C., & Zheng, L. (2023). High-entropy single-atom activated carbon catalysts for sustainable oxygen electrocatalysis. *Nature Sustainability, 6*(7), 816–826. https://doi.org/10.1038/s41893-023-01101-z

10 Qi, G., Wang, Q., Xiao, R., Zhang, H., & Zhou, Z. (2023). Microwave biochar produced with activated carbon catalyst: Characterization and adsorption of heavy metals. *Environmental Research, 216*, 114732. https://doi.org/10.1016/j.envres.2022.114732

11 Shan, R., Han, J., Gu, J., Yuan, H., Luo, B., & Chen, Y. (2020). A review of recent developments in catalytic applications of biochar-based materials. *Resources, Conservation and Recycling, 162*, 105036. https://doi.org/10.1016/j.resconrec.2020.105036

Buketov university

12 Poonia, K., Pradhan, D., Kulkarni, P.S., Saini, R., & Kothiyal, N.C. (2024). Sustainability, performance, and production perspectives of waste-derived functional carbon nanomaterials towards a sustainable environment: A review. *Chemosphere, 352*, 141419. https://doi.org/10.1016/j.chemosphere.2024.141419

13 Jan-Roblero, J., & Cruz-Maya, J.A. (2023). Ibuprofen: Toxicology and Biodegradation of an Emerging Contaminant. *Molecules, 28*(5), 2097. https://doi.org/10.3390/molecules28052097

14 Monteiro, C., Silvestre, S., Duarte, A.P., & Alves, G. (2022). Safety of Non-Steroidal Anti-Inflammatory Drugs in the Elderly: An Analysis of Published Literature and Reports Sent to the Portuguese Pharmacovigilance System. *International Journal of Environmental Research and Public Health, 19*(6), 3541. https://doi.org/10.3390/ijerph19063541

15 Parolini, M., Binelli, A., & Provini, A. (2011). Chronic effects induced by ibuprofen on the freshwater bivalve Dreissena polymorpha. *Ecotoxicology and Environmental Safety, 74*(6), 1586–1594. https://doi.org/10.1016/j.ecoenv.2011.04.025.

16 Marchlewicz, A., Guzik, U., & Wojcieszyńska, D. (2015). Over-the-Counter Monocyclic Non-Steroidal Anti-Inflammatory Drugs in Environment—Sources, Risks, Biodegradation. *Water, Air, & Soil Pollution, 226*(10), 355. https://doi.org/10.1007/s11270-015-2622-0.

17 Huang, H., & Liu, G. (2015). Ozone-Oxidation Products of Ibuprofen and Toxicity Analysis in Simulated Drinking Water. *Journal of Drug Metabolism & Toxicology, 6*(3). https://doi.org/10.4172/2157-7609.1000181.

18 Chopra, S., & Kumar, D. (2020). Ibuprofen as an emerging organic contaminant in environment, distribution and remediation. *Heliyon, 6*(6), e04087. https://doi.org/10.1016/j.heliyon.2020.e04087

19 Zaied, B.K., Rashid, M., Nasrullah, M., Zularisam, A.W., Pant, D., & Singh, L. (2020). A comprehensive review on contaminants removal from pharmaceutical wastewater by electrocoagulation process. *Science of The Total Environment, 726*, 138095. https://doi.org/10.1016/j.scitotenv.2020.138095

20 Brillas, E. (2022). A critical review on ibuprofen removal from synthetic waters, natural waters, and real wastewaters by advanced oxidation processes. *Chemosphere, 286*, 131849. https://doi.org/10.1016/j.chemosphere.2021.131849

21 Ayati, A., Tanhaei, B., Beiki, H., Krivoshapkin, P., Krivoshapkina, E., & Tracey, C. (2023). Insight into the adsorptive removal of ibuprofen using porous carbonaceous materials: A review. *Chemosphere, 323*, 138241. https://doi.org/10.1016/j.chemosphere.2023.138241

22 Costa, F.C.R., dos Santos, C.R., & Amaral, M.C.S. (2023). Trace organic contaminants removal by membrane distillation: A review on mechanisms, performance, applications, and challenges. *Chemical Engineering Journal, 464*, 142461. https://doi.org/10.1016/j.cej.2023.142461

23 The Food and Agriculture Organization of the United Nations (2024). GIEWS — Global Information and Early Warning System. *Country Briefs.* Kazakhstan. https://www.fao.org/giews/countrybrief/country.jsp? code=KAZ

24 Domingues, R.R., Trugilho, P.F., Silva, C.A., de Melo, I.C.N.A., Melo, L.C.A., Magriotis, Z.M., & Sánchez-Monedero, M.A. (2017). Properties of biochar derived from wood and high-nutrient biomasses with the aim of agronomic and environmental benefits. *PLOS ONE, 12(5)*, e0176884. https://doi.org/10.1371/journal.pone.0176884

25 ThermoFisher Scientific (2022). Spectrophotometric analysis of ibuprofen according to USP and EP monographs: Performing pharmaceutical identification tests with an Evolution UV-Visible Spectrophotometer [PDF]. ThermoFisher Scientific. https://assets.thermofisher.com/TFS-Assets/MSD/Application-Notes/AN53349-spectrophotometric-analysis-ibuprofen.pdf

26 Amerkhanova, S., Shlyapov, R., & Uali, A. (2017). The active carbons modified by industrial wastes in process of sorption concentration of toxic organic compounds and heavy metals ions. *Colloids and Surfaces A: Physicochemical and Engineering Aspects*, 532. https://doi.org/10.1016/j.colsurfa.2017.07.015

27 Rambabu, N., Rao, B.V.S.K., Surisetty, V.R., Das, U., & Dalai, A.K. (2015). Production, characterization, and evaluation of activated carbons from de-oiled canola meal for environmental applications. *Industrial Crops and Products, 65*, 572–581. https://doi.org/10.1016/j.indcrop.2014.09.046

28 Egirani, D., Latif, M.T., Wessey, N., Poyi, N.R., & Shehata, N. (2021). Preparation and characterization of powdered and granular activated carbon from Palmae biomass for mercury removal. *Applied Water Science, 11*(1), 10. https://doi.org/10.1007/s13201-020-01343-8

29 Rashidi, N.A., Yusup, S., Ahmad, M.M., Mohamed, N.M., & Hameed, B.H. (2012). Activated carbon from the renewable agricultural residues using single step physical activation: A preliminary analysis. *APCBEE Procedia, 3*, 84–92. https://doi.org/10.1016/j.apcbee.2012.06.051

30 Jun, T.Y., Arumugam, S.D., Latip, N.H.A., Abdullah, A.M., & Latif, P.A. (2010). Effect of Activation Temperature and Heating Duration on Physical Characteristics of Activated Carbon Prepared from Agriculture Waste. *Thai Society of Higher Education Institutes on Environmen. EnvironmentAsia, 3*, 143–148. https://doi.org/10.14456/ea.2010.53

31 Kookana, R.S., Sarmah, A.K., Van Zwieten, L., Krull, E., & Singh, B. (2011). Biochar Application to Soil (pp. 103–143). https://doi.org/10.1016/B978-0-12-385538-1.00003-2

32 Qian, K., Kumar, A., Patil, K., Bellmer, D., Wang, D., Yuan, W., & Huhnke, R. (2013). Effects of Biomass Feedstocks and Gasification Conditions on the Physiochemical Properties of Char. *Energies, 6*(8), 3972–3986. https://doi.org/10.3390/en6083972

33 Wei, S., Zhu, M., Fan, X., Song, J., Peng, P., Li, K., Jia, W., & Song, H. (2019). Influence of pyrolysis temperature and feedstock on carbon fractions of biochar produced from pyrolysis of rice straw, pine wood, pig manure and sewage sludge. *Chemosphere, 218*, 624–631. https://doi.org/10.1016/j.chemosphere.2018.11.177

34 Křikala, J., Diviš, P., Pořízka, J., Duborská, E., & Gajdušek, M. (2024). Application of biochar prepared from wheat bran as the binding phase in diffusive gradient in thin films technique for determination of mercury in natural waters. *Chemical Papers, 78*(6), 7815–7826. https://doi.org/10.1007/s11696-024-03635-8

Buketov University

35 Vaghela, D.R., & Others. (2023). Modelling and optimization of biochar-based adsorbent derived from wheat straw using response surface methodology on adsorption of Pb^{2+}. *International Journal of Environmental Research*, *17*(1). Springer Science and Business Media Deutschland GmbH. https://link.springer.com/article/10.1007/s41742-022-00498-3

36 Zhu, X., Qian, F., Liu, Y., Matera, D., Wu, G., Zhang, S., & Chen, J. (2016). Controllable synthesis of magnetic carbon composites with high porosity and strong acid resistance from hydrochar for efficient removal of organic pollutants: An overlooked influence. *Carbon*, *99*, 338–347. https://doi.org/10.1016/j.carbon.2015.12.044

37 Cazetta, A.L., Pezoti, O., Bedin, K.C., Silva, T.L., Paesano Junior, A., Asefa, T., & Almeida, V.C. (2016). Magnetic Activated Carbon Derived from Biomass Waste by Concurrent Synthesis: Efficient Adsorbent for Toxic Dyes. *ACS Sustainable Chemistry & Engineering*, *4*(3), 1058–1068. https://doi.org/10.1021/acssuschemeng.5b01141

38 Bedia, J., Peñas-Garzón, M., Gómez-Avilés, A., Rodriguez, J.J., & Belver, C. (2020). Review on Activated Carbons by Chemical Activation with $FeCl_3$. *C. Journal of Carbon Research*, *6*(2), 21. https://doi.org/10.3390/c6020021

39 Siburian, R., Sihotang, H., Lumban Raja, S., Supeno, M., & Simanjuntak, C. (2018). New Route to Synthesize of Graphene Nano Sheets. *Oriental Journal of Chemistry*, *34*(1), 182–187. https://doi.org/10.13005/ojc/340120

40 Liu, Y., Zhao, X., Li, J., Ma, D., & Han, R. (2012). Characterization of bio-char from pyrolysis of wheat straw and its evaluation on methylene blue adsorption. *Desalination and Water Treatment*, *46*(1–3), 115–123. https://doi.org/10.1080/19443994.2012.677408

41 Xu, Z., Zhang, T., Yuan, Z., Zhang, D., Sun, Z., Huang, Y., Chen, W., Tian, D., Deng, H., & Zhou, Y. (2018). Fabrication of cotton textile waste-based magnetic activated carbon using $FeCl_3$ activation by the Box–Behnken design: optimization and characteristics. *RSC Advances*, *8*(66), 38081–38090. https://doi.org/10.1039/C8RA06253F

42 Anabalón Fuentes, P., Kopp Pailañir, M., Rocha Mella, S., González Quijón, M.E., Marzialetti Bernardi, T., & Cea Lemus, M. (2024). Development of bifunctional biochar/iron oxide composites for tetracycline removal from synthetic wastewater. *Journal of Water Process Engineering*, *64*, 105509. https://doi.org/10.1016/j.jwpe.2024.105509

43 Yi, Y., Tu, G., Zhao, D., Tsang, P.E., & Fang, Z. (2020). Key role of FeO in the reduction of Cr(VI) by magnetic biochar synthesised using steel pickling waste liquor and sugarcane bagasse. *Journal of Cleaner Production*, *245*, 118886. https://doi.org/10.1016/j.jclepro.2019.118886

44 Özçimen, D., & Ersoy-Meriçboyu, A. (2010). Characterization of biochar and bio-oil samples obtained from carbonization of various biomass materials. *Renewable Energy*, *35*(6), 1319–1324. https://doi.org/10.1016/j.renene.2009.11.042

45 Reza, M.S., Afroze, S., Bakar, M.S.A., Saidur, R., Aslfattahi, N., Taweekun, J., & Azad, A.K. (2020). Biochar characterization of invasive Pennisetum purpureum grass: effect of pyrolysis temperature. *Biochar*, *2*(2), 239–251. https://doi.org/10.1007/s42773-020-00048-0

46 Barakat, N.A.M., Mahmoud, M.S., & Moustafa, H.M. (2024). Comparing specific capacitance in rice husk-derived activated carbon through phosphoric acid and potassium hydroxide activation order variations. *Scientific Reports*, *14*(1), 1460. https://doi.org/10.1038/s41598-023-49675-0

47 Chia, C.H., Gong, B., Joseph, S.D., Marjo, C.E., Munroe, P., & Rich, A.M. (2012). Imaging of mineral-enriched biochar by FTIR, Raman and SEM–EDX. *Vibrational Spectroscopy*, *62*, 248–257. https://doi.org/10.1016/j.vibspec.2012.06.006

48 Adeniyi, A.G., Adeyanju, C.A., Emenike, E.C., Otoikhian, S.K., Ogunniyi, S., Iwuozor, K.O., & Raji, A.A. (2022). Thermal energy recovery and valorisation of Delonix regia stem for biochar production. *Environmental Challenges*, *9*, 100630. https://doi.org/10.1016/j.envc.2022.100630

49 Anfar, Z., Zbair, M., Ait Ahsiane, H., Jada, A., & El Alem, N. (2020). Microwave assisted green synthesis of Fe_2O_3/biochar for ultrasonic removal of nonsteroidal anti-inflammatory pharmaceuticals. *RSC Advances*, 10(19), 11371–11380. https://doi.org/10.1039/d0ra00617c

50 Zhu, Q., Zhang, K., Xu, J., Wei, X., Shi, L., Sumita, Li, C., & Lichtfouse, E. (2023). Performance and Mechanism of Fe_3O_4 Loaded Biochar Activating Persulfate to Degrade Acid Orange 7. *Water*, 15(10), 1849. https://doi.org/10.3390/w15101849

51 Coimbra, R.N., Escapa, C., & Otero, M. (2018). Adsorption separation of analgesic pharmaceuticals from ultrapure and wastewater: Batch studies using a polymeric resin and an activated carbon. *Polymers*, *10*(9), 958. https://doi.org/10.3390/polym10090958

52 Jean-Rameaux, B., Brice, T., Sadou, D., Jean-Baptiste, T., Berthelot, S.T., Elie, A., Georges, K.Y., & Samuel, L. (2021). Multi-functionalized cellulosic biomass by plasma-assisted bonding of α-amino carboxylic acid to enhance the removal of ibuprofen in aqueous solution. *Journal of Polymers and the Environment*, *29*(4), 1176–1191. https://doi.org/10.1007/s10924-020-01958-7

53 Cao, Y., Nakhjiri, A.T., & Ghadiri, M. (2021). Numerical investigation of ibuprofen removal from pharmaceutical wastewater using adsorption process. *Scientific Reports*, *11*(1), 24478. https://doi.org/10.1038/s41598-021-04062-4

54 Chakraborty, P., Show, S., Banerjee, S., & Halder, G. (2018). Mechanistic insight into sorptive elimination of ibuprofen employing bi-directional activated biochar from sugarcane bagasse: Performance evaluation and cost estimation. *Journal of Environmental Chemical Engineering*, *6*(4), 5287–5300. https://doi.org/10.1016/j.jece.2018.08.017

55 Moreno-Pérez, J., Pauletto, P.S., Cunha, A.M., Bonilla-Petriciolet, A., Salau, N.P.G., & Dotto, G.L. (2021). Three-dimensional mass transport modeling of pharmaceuticals adsorption inside ZnAl/biochar composite. *Colloids and Surfaces A: Physicochemical and Engineering Aspects*, *614*, 126170. https://doi.org/10.1016/j.colsurfa.2021.126170

56 Ngernyen, Y., Petsri, D., Sribanthao, K., Kongpennit, K., Pinijnam, P., Pedsakul R., & Hunt, A. (2023). Adsorption of the non-steroidal anti-inflammatory drug (ibuprofen) onto biochar and magnetic biochar prepared from chrysanthemum waste of the beverage industry. *RSC Advances*, *13*(21), 14712–14728. https://doi.org/10.1039/D3RA01949G

Burapha University

57 Álvarez-Torrellas, S., Rodríguez, A., Ovejero, G., & García, J. (2016). Comparative adsorption performance of ibuprofen and tetracycline from aqueous solution by carbonaceous materials. *Chemical Engineering Journal, 283*, 936–947. https://doi.org/10.1016/j.cej.2015.08.023

58 Fröhlich, A.C., dos Reis, G.S., Pavan, F.A., Lima, É.C., Foletto, E.L., & Dotto, G.L. (2018). Improvement of activated carbon characteristics by sonication and its application for pharmaceutical contaminant adsorption. *Environmental Science and Pollution Research, 25*(25), 24713–24725. https://doi.org/10.1007/s11356-018-2525-x

59 Rabbat, C., Pinna, A., Andres, Y., Villot, A., & Awad, S. (2023). Adsorption of ibuprofen from aqueous solution onto a raw and steam-activated biochar derived from recycled textile insulation panels at end-of-life: Kinetic, isotherm, and fixed-bed experiments. *Journal of Water Process Engineering, 53*, 103830. https://doi.org/10.1016/j.jwpe.2023.103830

60 Nguyen, T.K.T., Nguyen, T.B., Chen, W.H., Chen, C.W., Patel, A.K., Bui, X.T., Chen, L., Singhania, R.R., & Dong, C.D. (2023). Phosphoric acid-activated biochar derived from sunflower seed husk: Selective antibiotic adsorption behavior and mechanism. *Bioresource Technology, 371*, 128593. https://doi.org/10.1016/j.biortech.2023.128593

61 Mestre, A.S., Pires, J., Nogueira, J.M.F., & Carvalho, A.P. (2007). Activated carbons for the adsorption of ibuprofen. *Carbon, 45*(10), 1979–1988. https://doi.org/10.1016/j.carbon.2007.06.005

62 Wang, G., Yong, X., Luo, L., Yan, S., Wong, J.W.C., & Zhou, J. (2022). Structure-performance correlation of high surface area and hierarchical porous biochars as chloramphenicol adsorbents. *Separation and Purification Technology, 296*, 121374. https://doi.org/10.1016/j.seppur.2022.121374

63 European Biochar Certificate (EBC) (2012–2023). European Biochar Certificate — Guidelines for a sustainable production of biochar (Version 10.3). Carbon Standards International (CSI). http://european-biochar.org

64 Mestre, A.S., Pires, J., Nogueira, J.M.F., & Carvalho, A.P. (2007). Activated carbons for the adsorption of ibuprofen. *Carbon, 45*(10), 1979–1988. https://doi.org/10.1016/j.carbon.2007.06.005

65 Wang, J., & Guo, X. (2020). Adsorption kinetic models: Physical meanings, applications, and solving methods. *Journal of Hazardous Materials, 390*, 122–156. https://doi.org/10.1016/j.jhazmat.2020.122156

66 Plazinski, W., Rudzinski, W., & Plazinska, A. (2009). Theoretical models of sorption kinetics including a surface reaction mechanism: A review. *Advances in Colloid and Interface Science, 152*(1–2), 2–13. https://doi.org/10.1016/j.cis.2009.07.009

67 Surela, A.K., Chhachhia, L.K., Surela, V.K., & Meena, P.L. (2024). Polypyrrole-Based Composites for Dyes Removal From Contaminated Water. In *Reference Module in Materials Science and Materials Engineering*. Elsevier. https://doi.org/10.1016/B978-0-323-95486-0.00019-3

68 Ramírez-Rodríguez, T., & de Landa Castillo-Alvarado, F. (2012). Application of the intra-particle diffusion model for activated carbon fibers in an aqueous medium. *MRS Proceedings, 1373*, imrc-1373-s4-24. https://doi.org/10.1557/opl.2012.311

69 Pezoti, O., Cazetta, A.L., Souza, I.P.A.F., Bedin, K.C., Martins, A.C., Silva, T.L., & Almeida, V.C. (2014). Adsorption studies of methylene blue onto $ZnCl_2$-activated carbon produced from buriti shells (*Mauritia flexuosa* L.). *Journal of Industrial and Engineering Chemistry, 20*(6), 4401–4407. https://doi.org/10.1016/j.jiec.2014.02.007

70 Ghaedi, M., Golestani Nasab, A., Khodadoust, S., Rajabi, M., & Azizian, S. (2014). Application of activated carbon as adsorbents for efficient removal of methylene blue: Kinetics and equilibrium study. *Journal of Industrial and Engineering Chemistry, 20*(4), 2317–2324. https://doi.org/10.1016/j.jiec.2013.10.007

71 Villabona-Ortíz, Á., Tejada-Tovar, C., & Ortega-Toro, R. (2021). Kinetics and adsorption isotherms of the removal of ibuprofen on a porous adsorbent made from agroindustrial waste. *Desalination and Water Treatment, 209*, 316–323. Desalination Publications. https://doi.org/10.5004/dwt.2021.27515

72 World Health Organization (1999). Guidelines for safe disposal of unwanted pharmaceuticals in and after emergencies. https://www.who.int/publications/i/item/guidelines-for-safe-disposal-of-unwanted-pharmaceuticals-in-and-after-emergencies

Buketov University